

Short Communication

Phase engineering of H/T-Nb₂O₅ homojunction for enhanced lithium-ion storageSheng Li^{a,b}, Jun Li^b, Wenjie Zhang^b, Sherif A. El-Khodary^b, Yubo Luo^a, Dickon H.L. Ng^c, Xiaoshui Peng^c, Jiabiao Lian^{b,*}^a State Key Laboratory of Material Processing and Die & Mould Technology, School of Materials Science and Engineering, Huazhong University of Science and Technology, Wuhan 430074, China^b Institute for Energy Research, Jiangsu University, Zhenjiang 212013, China^c School of Science and Engineering, The Chinese University of Hong Kong (Shenzhen), Shenzhen 518172, China

ARTICLE INFO

Keywords:

Phase engineering
Monoclinic/Rthorhombic
Nb₂O₅ homojunction
Kinetics analysis
Li-ion storage

ABSTRACT

Phase engineering has gained significant attention in energy-storage applications due to its ability to tailor the physicochemical properties and functionalities of electrode materials. In this study, we demonstrate the in-situ partial phase conversion of niobium pentoxide (Nb₂O₅), resulting in the formation of a monoclinic/orthorhombic (H/T-Nb₂O₅) heterophase homojunction. This study further confirms that the unique heterophase interface plays a crucial role in regulating the local electronic environment, resulting in charge redistribution, the formation of an internal electric field, and enhanced electron transfer. Moreover, the presence of abundant phase interfaces offers additional reactive sites for Li⁺ ion adsorption, thereby enhancing reaction dynamics. The synergistic effects within the H/T-Nb₂O₅ homojunction are reflected in its high Li⁺ storage capacity (413 mAh g⁻¹ at 100 mA g⁻¹), superior rate capability, and cycling stability. Thus, this study demonstrates that the construction of heterophase homojunctions offers a promising strategy for developing high-performance anode materials for efficient Li-ion storage.

1. Introduction

Lithium-ion batteries (LIBs) are the main power sources for portable electronic devices and electric vehicles [1–3]. However, traditional graphite-based LIBs face persistent challenges such as slow charge/discharge rate and lithium dendrite formation [4–6], which compromise safety and performance. As a result, there is an urgent need to develop advanced anode materials for safer and more efficient LIBs. Nb₂O₅, a typical intercalation-type transition metal oxide (TMO), has emerged as a promising anode material due to its high work potential, excellent chemical stability, and abundant resources [7,8]. Nonetheless, Nb₂O₅ suffers from slow lithium-ion kinetics at high rates, leading to significant polarization and limiting its effectiveness in reversible lithium storage [9,10]. To address these limitations, extensive research has focused on improving the reaction kinetics of Nb₂O₅ to promote its electrochemical performance. Key strategies include: (i) fabricating nano- and micro-architectures with unique morphologies to increase the contact area with the electrolyte and shorten the path length of Li⁺ diffusion [11,12], (ii) incorporating highly conductive carbon matrices to prevent self-aggregation and enhance structural stability [13], and (iii) introducing defects to provide active sites and reduce the Li⁺ diffusion energy

barrier [14]. Despite improvements in structural stability and electrical conductivity through morphology engineering and coating strategies, the intrinsic slow electrochemical reaction activity of Nb₂O₅ remains a challenge. This issue has deterred its industrial adoption due to unreliable processing methods. Therefore, developing effective strategies to enhance the rate performance and capacity of Nb₂O₅ is critical for advancing LIB technology.

The crystal phases of nanomaterials strongly influence their physicochemical properties and functionalities. Therefore, tailoring phase transformations is a feasible approach to enhancing the electrochemical performance of electrode materials [15–18]. For instance, Song et al. demonstrated that cubic/orthorhombic-CoSe₂ phase-junctions via chemical vapor deposition, facilitated homogeneous interfacial electronic migration and ion diffusion, thereby improving electrochemical reaction kinetics for sodium and potassium storage [19]. Similarly, Cao et al. synthesized different crystal phases of Mn_xCo_{1-x}O using a cation regulation strategy, which enhanced the electrical and catalytic properties of Li-O₂ batteries [20]. Inspired by these studies, we explored the properties of Nb₂O₅ with different crystal phases to study the impact of the phase structure on its electrochemical performance. Nb₂O₅ typically possesses two structural phases: the orthorhombic phase

* Corresponding author.

E-mail address: jblian@ujs.edu.cn (J. Lian).<https://doi.org/10.1016/j.chphma.2024.09.002>

Received 17 May 2024; Received in revised form 7 September 2024; Accepted 17 September 2024

Available online 25 September 2024

2772-5715/© 2024 The Authors. Publishing Services by Elsevier B.V. on behalf of KeAi Communications Co. Ltd. This is an open access article under the CC BY-NC-ND license (<http://creativecommons.org/licenses/by-nc-nd/4.0/>)

(T-Nb₂O₅) and monoclinic phase (H-Nb₂O₅) [21,22]. The distinct crystallographic structure of these phases significantly influences their electrochemical properties. Therefore, constructing a heterophase homojunction with these two phases offers a promising strategy for achieving excellent electrochemical performance of Nb₂O₅-based electrodes.

In this study, we designed orthorhombic/monoclinic Nb₂O₅ (H/T-Nb₂O₅) homojunctions through partial phase transformation at a specific temperature. This approach combines the unique advantages of the orthorhombic and monoclinic phases. At the homojunction interfaces, the spontaneous imbalance in charge distribution creates an internal electric field promoting interfacial charge transport and providing additional reactive sites. Consequently, the H/T-Nb₂O₅ homojunction exhibits superior electrochemical performance. Our findings offer valuable insights into the application of crystal phase engineering in the development of advanced energy storage.

2. Materials and methods

2.1. Preparation of H-Nb₂O₅, H/T-Nb₂O₅ and T-Nb₂O₅ microflowers

All chemicals used in this study were analytical reagents and were used without purification. Initially, 7.5 mmol of niobium oxalate (C₁₀H₅NbO₂₀) and 1.5 mmol of ammonium carbonate ((NH₄)₂CO₃) were added to 30 mL of deionized water. The mixture was sonicated for 30 min. The resulting suspension was then transferred to a Teflon-lined stainless-steel autoclave (50 mL) and heated at 200 °C for 12 h. Thereafter, the product was collected, washed, and dried to obtain monoclinic-Nb₂O₅ (H-Nb₂O₅) sample.

To obtain orthorhombic-Nb₂O₅ (T-Nb₂O₅), the H-Nb₂O₅ sample was annealed at 700 °C for 1 h in air.

The H/T-Nb₂O₅ sample was obtained by annealing the H-Nb₂O₅ sample at 500 °C for 1 h in air.

2.2. Characterization

Powder X-ray diffraction (XRD, German Bruker D8 diffractometer) with Cu radiation was used to characterize the crystalline structure of the samples. The morphologies and microstructures of the materials were studied using field-emission scanning electron microscopy (FE-SEM, JEOL, JSM-7800F) and high-resolution transmission electron microscopy (HRTEM, FEI Tecnai G2 F30 S-Twin TEM). X-ray photoelectron spectroscopy (XPS, Thermo Scientific ESCALAB 250Xi system with a monochromated Al K α X-ray source 1486.6 eV) was used to measure the surface elemental composition and chemical states of the samples.

2.3. Electrochemical measurements

The electrode preparation involved dispersing Nb₂O₅ microflowers (80 wt.%), super conductive carbon black (SCCB, Ketjenblack EC-600JD, Lion Corporation) (10 wt.%), and polyvinylidene fluoride (PVDF) (10 wt.%) in N-methyl-2-pyrrolidone (NMP). The resulting slurry was then coated onto copper foil as a current collector. The loading mass ranged from 1.0 to 1.2 mg cm⁻². Lithium metal served as both the reference and counter electrode, with a 1 M LiPF₆ EC/DMC/DC electrolyte solution and a Celgard 2400 porous polypropylene membrane as the separator. CR2032-type coin cells were assembled in an Ar-filled glovebox (O₂/H₂O < 0.01 ppm) for electrochemical testing. Cyclic voltammetry (CV) was performed within the potential window of 0.01–3.00 V vs Li/Li⁺, and electrochemical impedance spectroscopy (EIS) measurements were performed using an AC perturbation of 5 mV on a Gamry Interface 1000E Potentiostat. Galvanostatic discharge/charge and galvanostatic intermittent titration technique (GITT) tests (at 0.1 A g⁻¹, with pulse time of 5 min and 1 h rest intervals) were conducted using the NEWARE-CT-4008 battery testing system.

3. Results and discussion

Fig. 1 shows the FE-SEM and TEM images of H-Nb₂O₅ (Figs. 1(a)(d)) and H/T-Nb₂O₅ (Figs. 1(b)(e)), which reveal their microflower structures composed of nanosheets. In contrast, T-Nb₂O₅ exhibits a coral-like morphology (Figs. 1(c)(f)), resulting from a phase transition induced by high-temperature treatment. Their microstructures were further observed using HRTEM (Figs. 1(g)–(i)). As shown in Fig. 1(g), H-Nb₂O₅ exhibits a lattice spacing of 0.358 nm, corresponding to the (121) plane of the monoclinic phase [13]. The (200) plane of T-Nb₂O₅ with a lattice spacing of 0.309 nm is shown in Fig. 1(i) [23]. Fig. 1(h) shows the lattice spacings for both H-Nb₂O₅ (0.358 nm) and T-Nb₂O₅ (0.309 nm), confirming the successful formation of a heterohomojunction with intimate contact between the orthorhombic and monoclinic phases.

Fig. 2(a) shows the crystal structure features and phase purity of Nb₂O₅ obtained using XRD. The diffraction peaks of H-Nb₂O₅ correspond to the standard monoclinic phase (PDF No 19–0862) [13,21], whereas the peaks for T-Nb₂O₅ match the orthorhombic phase (PDF No 27–1003) [24]. The absence of additional peaks indicates the high phase purity of the sample. As expected, the diffraction peaks of H/T-Nb₂O₅ indicate the coexistence of monoclinic and orthorhombic phases. The HRTEM and XRD results demonstrate the successful phase modulation of Nb₂O₅ samples. XPS was employed to characterize the chemical states of Nb₂O₅ in different samples. The survey spectra revealed strong Nb and O signals in Nb₂O₅ (Fig. S1). The Nb 3d core-level spectrum of H/T-Nb₂O₅ in Fig. 2(b) shows two characteristic peaks at 209.9 and 207.2 eV, corresponding to Nb 3d3/2 and Nb 3d5/2 for Nb⁵⁺ [14,25]. A shift toward lower binding energies in both H/T-Nb₂O₅ and T-Nb₂O₅ spectra suggests electron migration and a strong coupling effect [14]. The high-resolution O 1s spectra (Fig. 2(c)) show a dominant peak at 530.3 eV, attributed to the O–Nb bond, and a peak at 531.4 eV associated with oxygen defects [26]. The heterophase structure of H/T-Nb₂O₅ is expected to deliver enhanced electrochemical performance.

To investigate the Li⁺ storage behavior of Nb₂O₅ with different crystal structures, CV tests were conducted at a scan rate of 0.1 mV s⁻¹ and galvanostatic charge-discharge (GCD) tests were performed at 0.1 A g⁻¹ within a potential window of 0.01–3.0 V (Fig. S2). Fig. S2(a) shows the initial three CV cycles of H/T-Nb₂O₅. In the first cathodic sweep, three prominent peaks were observed at 2.1, 1.3, and 0.65 V. The peaks at 2.1 and 1.3 V (broad) correspond to the intercalation of Li⁺ ions into Nb₂O₅ (Nb₂O₅ + xLi⁺ + xe⁻ ↔ Li_xNb₂O₅) [27]. The irreversible cathodic peak at 0.64 V, resulting from the formation of a solid electrolyte interphase (SEI), disappeared in subsequent cycles [28,29]. During the anodic process, a single peak at 1.75 V indicated delithiation [22].

Fig. 3(a) shows the integrated CV curves of the Nb₂O₅ electrode. It is evident that broad cathodic and anodic peaks appeared at 1.55/1.75 V, 1.38/1.64 V, and 1.66/1.87 V for H/T-Nb₂O₅, H-Nb₂O₅, and T-Nb₂O₅ electrodes, respectively, corresponding to the reversible Li⁺ insertion/extraction during discharge/charge cycles. Among the electrodes, the H/T-Nb₂O₅ exhibited the smallest potential difference of approximately 0.2 V, indicating lower polarization and higher Li⁺ kinetics compared to the other two electrodes [30]. Notably, Fig. 3(a) shows that the main capacity contribution potential intervals differed between the electrodes: H-Nb₂O₅ primarily contributed below 1.5 V, while T-Nb₂O₅ contributed above 1.2 V. These differences in Li⁺ storage potential window were also apparent in their GCD profiles at 0.1 A g⁻¹ (Fig. 3(b)). Thus, the H/T-Nb₂O₅ heterophase homojunction combined the advantages of H-Nb₂O₅ and T-Nb₂O₅, demonstrating superior Li⁺ storage performance. Fig. 3(c) presents the rate and cycling performances of the three electrodes. The H/T-Nb₂O₅ homojunction delivered excellent reversible capacities of 413, 333, 287, 247, 201, and 146 mAh g⁻¹ at 0.1, 0.25, 0.5, 1.0, 2.5, and 5.0 A g⁻¹, respectively. The corresponding GCD profiles (Fig. S3) indicate that the H/T-Nb₂O₅ homojunction electrode exhibited less polarization with increasing current density. Furthermore, the H/T-Nb₂O₅ homojunction maintained a reversible capacity of 236 mAh g⁻¹ with a capacity retention of 92% after 600 cycles at 1.0 A g⁻¹.

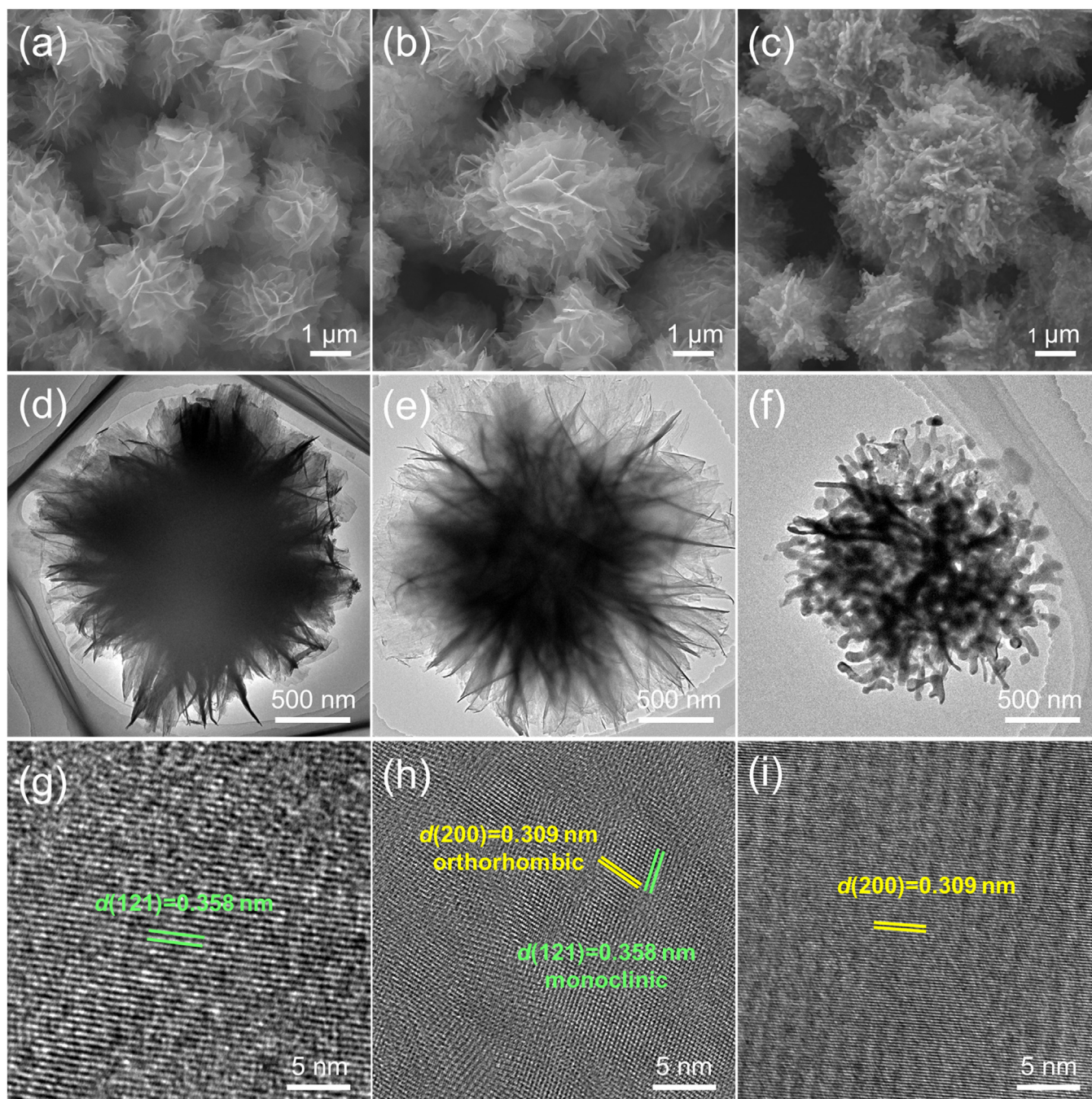


Fig. 1. Morphological characterization of Nb_2O_5 samples. FE-SEM, TEM, and HRTEM images of H- Nb_2O_5 (a)(d)(g), H/T- Nb_2O_5 (b)(e)(h) and T- Nb_2O_5 (c)(f)(i), respectively.

In contrast, the H- Nb_2O_5 and T- Nb_2O_5 electrodes showed inferior rate performance (55 and 92 mAh g^{-1} at 5.0 A g^{-1}) and cycling performances (76% and 78% retention at 1.0 A g^{-1}). This highlights the superiority of the designed H/T- Nb_2O_5 homojunction, which can be attributed to the built-in electric field at the intimate interface that enhances electron/ion transport, effectively reducing electrode polarization and accelerating reaction kinetics at high current densities. As summarized in Table S1, the rate capability and cycling stability of H/T- Nb_2O_5 surpass those of previously reported Nb_2O_5 -based anodes.

CV profiles at scan rates ranging from 0.1 to 5.0 mV s^{-1} were investigated to explore the Li^+ storage kinetics. The CV and b -value analyses are shown in Fig. S4, with additional details provided in the Sup-

plementary Materials. To gain deeper insights into the enhanced electron/ion transfer kinetics of the H/T- Nb_2O_5 homojunction, EIS and the galvanostatic intermittent titration technique (GITT) were employed. Fig. 4(a) displays the Nyquist plots of the Nb_2O_5 electrodes, where a semicircle in the high-frequency region corresponds to the charge transfer resistance (R_{ct}) and a line in the low-frequency region corresponds to the Warburg impedance (Z_w). The R_{ct} value of H/T- Nb_2O_5 is lower than that of H- Nb_2O_5 and T- Nb_2O_5 , indicating faster electron transfer at the phase interface, thereby reducing charge-transfer resistance [19]. Fig. 4(b) shows the $Z' - \omega^{-1/2}$ plots, where the slope of the fitted lines represents the Warburg impedance coefficient (σ_w). The smaller σ_w value for H/T- Nb_2O_5 suggests easier Li^+ diffusion within the elec-

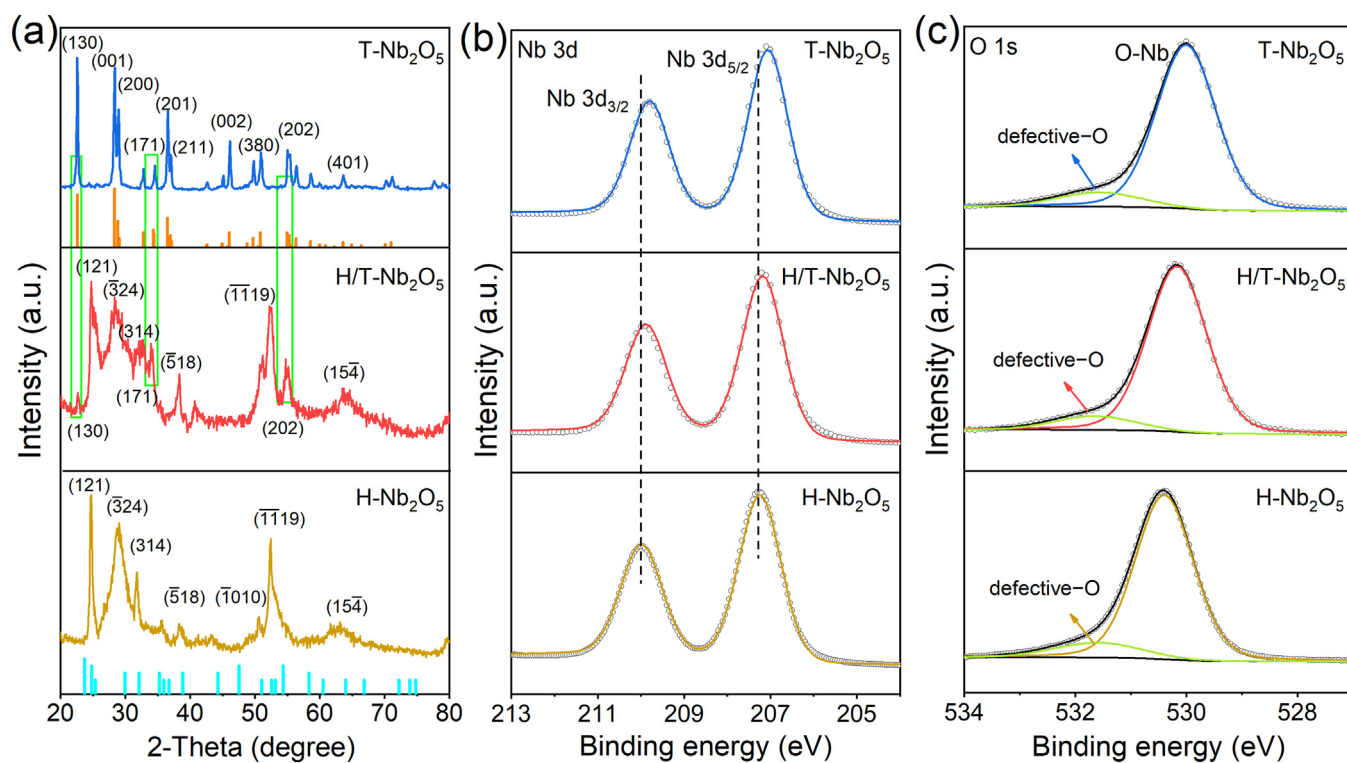


Fig. 2. Structural characterization of Nb₂O₅ samples. (a) XRD patterns. High-resolution XPS spectra of (b) Nb 3d and (c) O 1s.

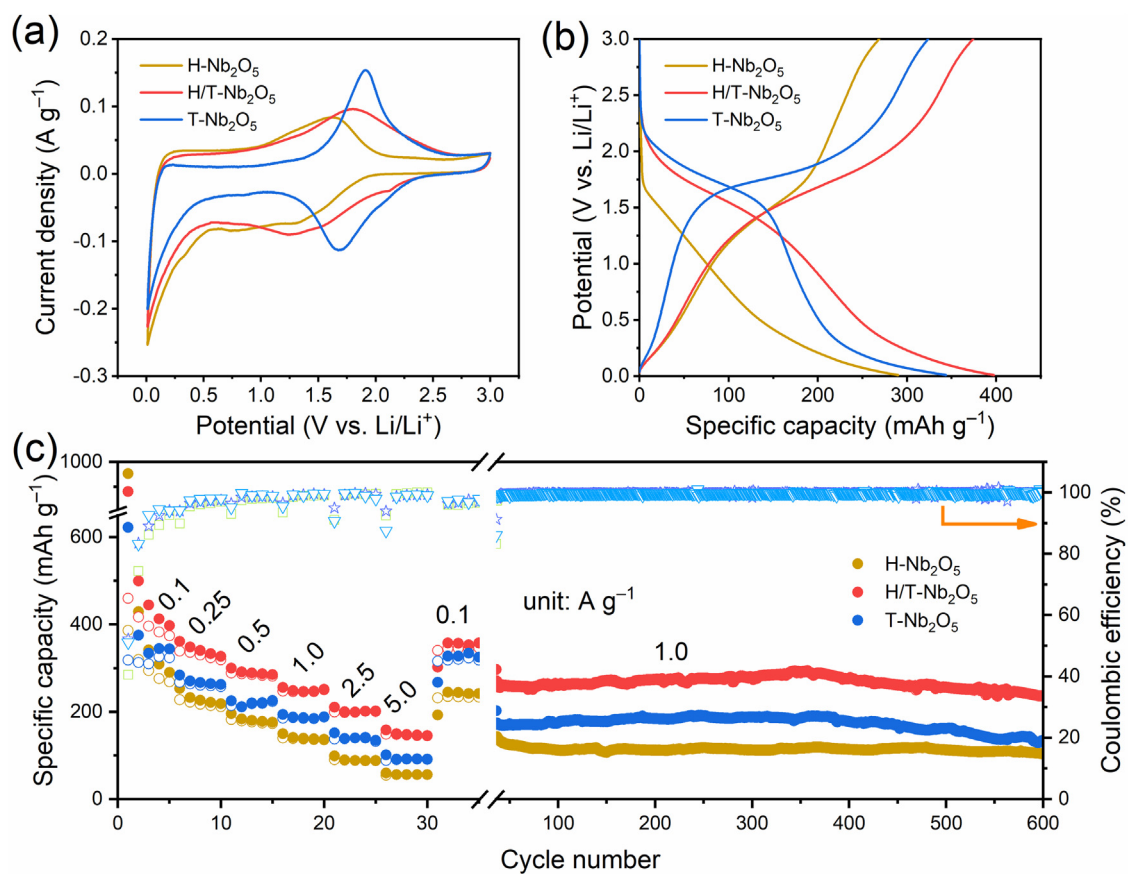


Fig. 3. Electrochemical properties of the Nb₂O₅ electrodes. (a) Integrated CV curves at 0.1 mV s⁻¹. (b) Integrated discharge-charge profiles at 0.1 A g⁻¹. (c) Rate and cycling performance.

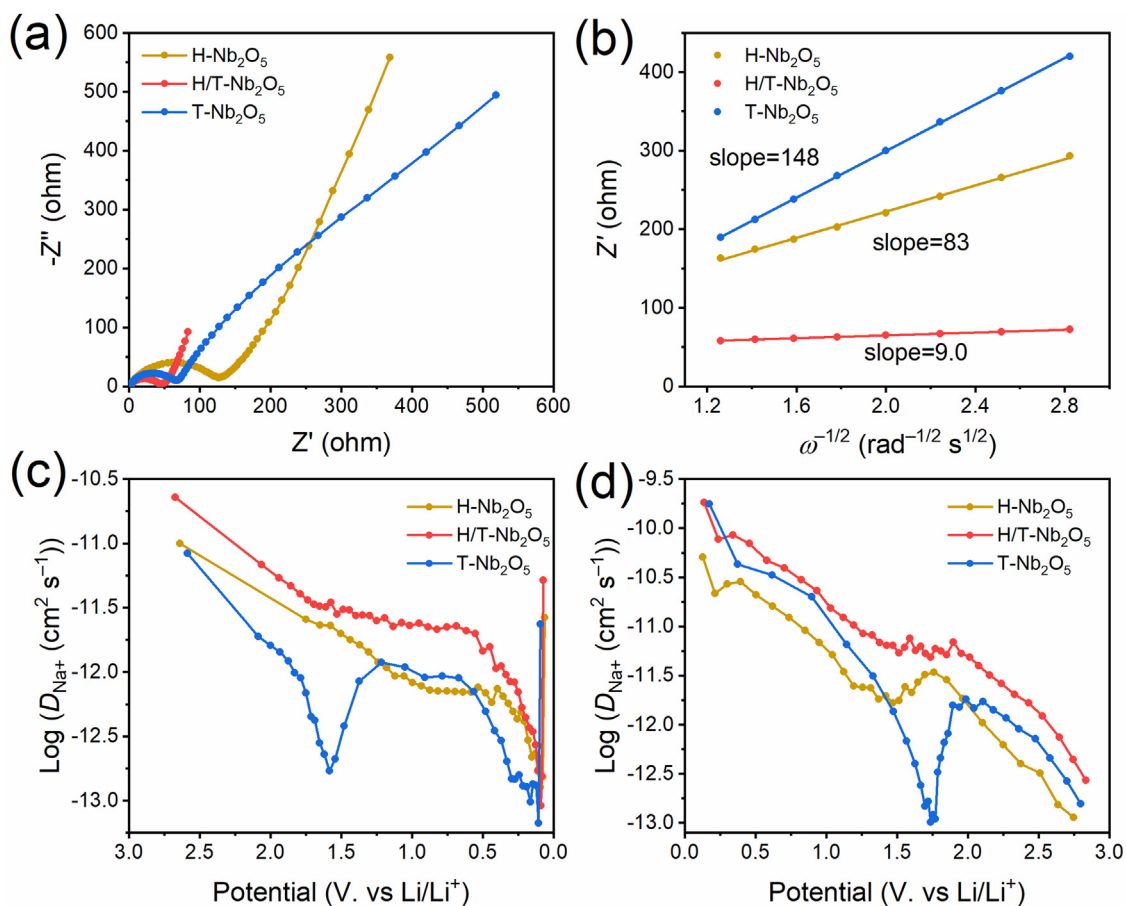


Fig. 4. Kinetic analyses of the Nb₂O₅ electrodes. (a) Nyquist plots. (b) $Z'-\omega^{-1/2}$ plots. (c) Lithium-ion diffusion coefficients in the discharge process and (d) charge process.

trode. These results were further validated by GITT (Fig. S5(a)), where the H/T-Nb₂O₅ electrode exhibited longer cycle times, implying higher capacity. A detailed enlarged pulse curve is shown in Fig. S5(b). The calculated diffusion coefficient (D_{Li^+}) values for the Nb₂O₅ electrodes during lithiation and delithiation are plotted in Figs. 4(c)(d), respectively. All three electrodes exhibited significant plateaus during the charge-discharge process, consistent with the peaks observed in the CV curves. Notably, Li⁺ diffusion in H/T-Nb₂O₅ was faster than in H-Nb₂O₅ and T-Nb₂O₅. The lower resistance and improved diffusion kinetics contributed to the significantly better rate performance of the H/T-Nb₂O₅ homojunction.

4. Conclusions

In this study, a unique H/T-Nb₂O₅ heterophase homojunction was successfully synthesized through a simple heat treatment process. The homogeneous interface induced a built-in electric field, which significantly enhanced charge-transfer kinetics. This hetero-phase homojunction demonstrated high specific capacity and rate capability, achieving 413 mAh g⁻¹ at 0.1 A g⁻¹ and 146 mAh g⁻¹ at 5.0 A g⁻¹. This study provides a promising strategy for improving electrochemical performance through phase engineering.

Declaration of Competing Interest

The authors declare that they have no known competing financial interests or personal relationships that could have appeared to influence the work reported in this paper.

CRediT authorship contribution statement

Sheng Li: Writing – original draft, Formal analysis, Data curation. **Jun Li:** Formal analysis, Data curation. **Wenjie Zhang:** Writing – review & editing, Formal analysis. **Sherif A. El-Khodary:** Funding acquisition, Formal analysis. **Yubo Luo:** Supervision. **Dickon H.L. Ng:** Writing – review & editing. **Xiaoshui Peng:** Writing – review & editing. **Jiabiao Lian:** Writing – review & editing, Supervision, Funding acquisition, Conceptualization.

Acknowledgements

We gratefully acknowledge financial support from the National Natural Science Foundation of China (22250410272 and 21706103) and the Natural Science Foundation of Jiangsu Province (BK20170549). D.H.L. Ng and X.S. Peng also express their gratitude for the Shenzhen Pengcheng Peacock Talent Scheme. J.B. Lian. extends sincere appreciation to the Jiangsu Provincial Program for High-Level Innovative and Entrepreneurial Talent Introduction.

Supplementary materials

Supplementary material associated with this article can be found, in the online version, at doi:10.1016/j.chphma.2024.09.002.

References

- [1] R.F. Service, Lithium-ion battery development takes Nobel, *Science* 366 (2019) 292.
- [2] H. Zhao, F. Yang, C.X. Li, T. Li, S.X. Zhang, C.X. Wang, Z.W. Zhang, R.T. Wang, Progress and perspectives on two-dimensional silicon anodes for lithium-ion batteries, *ChemPhysMater* 2 (2023) 1–19.

- [3] S.J. Zhang, Z.L. Qin, Z.G. Hou, J.J. Ye, Z.B. Xu, Y.T. Qian, Large-scale preparation of black phosphorus by molten salt method for energy storage, *ChemPhysMater* 1 (2022) 1–5.
- [4] L.Q. Zhang, C.X. Zhu, S.C. Yu, D.H. Ge, H.S. Zhou, Status and challenges facing representative anode materials for rechargeable lithium batteries, *J. Energy Chem.* 66 (2022) 260–294.
- [5] S. Fang, D. Bresser, S. Passerini, Transition metal oxide anodes for electrochemical energy storage in lithium-and sodium-ion batteries, *Adv. Energy Mater.* (2019) 55–99.
- [6] S.J. An, J.L. Li, C. Daniel, D. Mohanty, S. Nagpure, D.L. Wood, The state of understanding of the lithium-ion-battery graphite solid electrolyte interphase (SEI) and its relationship to formation cycling, *Carbon* 105 (2016) 52–76.
- [7] Z.H. Song, H. Li, W. Liu, H.Z. Zhang, J.W. Yan, Y.F. Tang, J.Y. Huang, H.M. Zhang, X.F. Li, Ultrafast and stable Li-(De) intercalation in a large single crystal H-Nb₂O₅ anode via optimizing the homogeneity of electron and ion transport, *Adv. Mater.* 32 (2020) 2001001.
- [8] T. Tian, L.L. Lu, Y.C. Yin, F. Li, T.W. Zhang, Y.H. Song, Y.H. Tan, H.B. Yao, Multiscale designed niobium titanium oxide anode for fast charging lithium-ion batteries, *Adv. Funct. Mater.* 31 (2020) 2007419.
- [9] F. Shen, Z.T. Sun, L. Zhao, Y.H. Xia, Y.Y. Shao, J.S. Cai, S. Li, C. Lu, X.L. Tong, Y. Zhao, J.Y. Sun, Y.L. Shao, Triggering the phase transition and capacity enhancement of Nb₂O₅ for fast-charging lithium-ion storage, *J. Mater. Chem. A* 9 (2021) 14534–14544.
- [10] X.Y. Han, P.A. Russo, N.G. Bretesché, S. Patané, S. Santangelo, R. Zhang, N. Pinna, Exploiting the condensation reactions of acetophenone to engineer carbon-encapsulated Nb₂O₅ nanocrystals for high-performance Li and Na energy storage systems, *Adv. Energy Mater.* 9 (2019) 1902813.
- [11] H.S. Li, Y. Zhu, S.Y. Dong, L.F. Shen, Z.J. Chen, X.G. Zhang, G.H. Yu, Self-assembled Nb₂O₅ nanosheets for high energy-high power sodium ion capacitors, *Chem. Mater.* 28 (2016) 5753–5760.
- [12] K. Kim, M.S. Kim, P.R. Cha, S.H. Kang, J.H. Kim, Structural modification of self-organized nanoporous niobium oxide via hydrogen treatment, *Chem. Mater.* 28 (2016) 1453–1461.
- [13] S.Y. Li, T. Wang, W.Q. Zhu, J.B. Lian, Y.P. Huang, Y.Y. Yu, J.X. Qiu, Y. Zhao, Y.C. Yong, H.M. Li, Controllable synthesis of uniform mesoporous H-Nb₂O₅/rGO nanocomposites for advanced lithium-ion hybrid supercapacitors, *J. Mater. Chem. A* 7 (2019) 693–703.
- [14] S. Li, Y.X. Cui, R. Kang, B.B. Zou, D.H.L. Ng, S.A.E. Khodary, X.H. Liu, J.X. Qiu, J.B. Lian, H.M. Li, Oxygen vacancies boosted the electrochemical kinetics of Nb₂O_{5-x} for superior lithium storage, *Chem. Commun.* 57 (2021) 8182–8185.
- [15] H.X. Li, X.C. Zhou, W. Zhai, S.Y. Lu, J.Z. Liang, Z. He, H.W. Long, T.F. Xiong, H.Y. Sun, Q.Y. He, Z.X. Fan, H. Zhang, Phase engineering of nanomaterials for clean energy and catalytic applications, *Adv. Energy Mater.* 10 (2020) 2002019.
- [16] Y. Chen, Z.C. Lai, X. Zhang, Z.X. Fan, Q.Y. He, C.L. Tan, H. Zhang, Phase engineering of nanomaterials, *Nat. Rev. Mater.* 4 (2020) 243–256.
- [17] Z.D. Lei, J. Zhan, L. Tang, Y. Zhang, Y. Wang, Recent development of metallic (1T) phase of molybdenum disulfide for energy conversion and storage, *Adv. Energy Mater.* 8 (2018) 1703482.
- [18] Y.F. Cao, S.C. Huang, Z.Q. Peng, F. Yao, X.H. Li, Y. Liu, H.T. Huang, M.M. Wu, Phase control of ultrafine fese nanocrystals in a N-doped carbon matrix for highly efficient and stable oxygen reduction reaction, *J. Mater. Chem. A* 9 (2019) 3464–3471.
- [19] X.F. Li, D. Pan, J. Deng, R. Wang, J.Z. Huang, W.M. L., T. Ya, X.J. Wang, Y.M. Zhang, L.L. Xu, Y. Bai, P. Xu, B. Song, Phase-junction engineering boosts the performance of CoSe₂ for efficient sodium/potassium storage, *J. Mater. Chem. A* 9 (2021) 25954–25963.
- [20] D. Cao, L. Zheng, Q.J. Li, J.F. Zhang, Y. Dong, J.S. Yue, X.R. Wang, Y. Bai, G.Q. Tan, C. Wu, Crystal phase-controlled modulation of binary transition metal oxides for highly reversible Li–O₂ batteries, *Nano Lett.* 21 (2021) 5225–5232.
- [21] S.Q. Guo, X. Zhang, Z. Zhou, G.D. Gao, L. Liu, Facile Preparation of hierarchical Nb₂O₅ microspheres with photocatalytic activities and electrochemical properties, *J. Mater. Chem. A* 2 (2014) 9236–9243.
- [22] T.T. Li, G. Nam, K.T. Liu, J.H. Wang, B. Zhao, Y. ding, L. Soule, M. Avdeev, Z.Y. Luo, W.L. Zhang, T. Yuan, P.P. Jing, M.G. Kim, Y.Y. Song, M.L. Liu, A niobium oxide with a shear structure and planar defects for high-power lithium-ion batteries, *Energy Environ. Sci.* 15 (2022) 254–264.
- [23] S.M. Zhang, G.L. Liu, W.M. Qiao, J.T. Wang, L.C. Ling, Oxygen vacancies enhance the lithium-ion intercalation pseudocapacitive properties of orthorhombic niobium pentoxide, *J. Colloid Interf. Sci.* 562 (2020) 193–203.
- [24] L.P. Yang, Y.E. Zhu, J. Sheng, F. Li, B. Tang, Y. Zhang, Z. Zhou, T-Nb₂O₅/C nanofibers prepared through electrospinning with prolonged cycle durability for high-rate sodium-ion batteries induced by pseudo-capacitance, *Small* 13 (2017) 1702588.
- [25] S. Cheng, J. Wang, S.R. Duan, J. Zhang, Q. Wang, Y. Zhang, L.G. Li, H.T. Liu, Q.B. Xiao, H.Z. Lin, Anionic oxygen vacancies in Nb₂O_{5-x}/Carbon hybrid host endow rapid catalytic behaviors for high-performance high areal loading lithium sulfur pouch cell, *Chem. Eng. J.* 417 (2021) 128172.
- [26] Q.M. Gan, H.N. He, K.M. Zhao, Z. He, S.Q. Liu, S.P. Yang, Plasma-induced oxygen vacancies in urchin-like anatase titania coated by carbon for excellent sodium-ion battery anodes, *ACS Appl. Mater. Interfaces.* 10 (2018) 7031–7042.
- [27] Z.Q. Hu, Q. He, Z.A. Liu, X. Liu, M.S. Qin, B. Wen, W.C. Shi, Y. Zhao, Q. Li, L.Q. Mai, Facile formation of tetragonal-Nb₂O₅ microspheres for high-rate and stable lithium storage with high areal capacity, *Sci. Bull.* 65 (2020) 1154–1162.
- [28] Z.C. Liu, W.J. Dong, J.B. Wang, C.L. Dong, Y. Lin, I.W. Chen, F.Q. Huang, Orthorhombic Nb₂O_{5-x} for durable high-rate anode of Li-ion batteries, *iScience* 23 (2020) 100767.
- [29] H. Park, D. Lee, T. Song, High capacity monoclinic Nb₂O₅ and semiconducting NbO₂ composite as high-power anode material for Li-ion batteries, *J. Power Sources.* 414 (2019) 377–382.
- [30] Y.J. Zheng, Z.G. Yao, Z. Shadike, M. Lei, J.J. Liu, C.L. Li, Defect-concentration-mediated T-Nb₂O₅ anodes for durable and fast-charging Li-ion batteries, *Adv. Funct. Mater.* 32 (2022) 2107060.